

# A Comparative Analysis of Structural and Electrochemical Properties of Graphene Oxide (GO) and Reduced Graphene Oxide (rGO) Synthesized by Using Hummer's and Modified Hummer's Method

S. Das<sup>1</sup>, R. Ghadai<sup>1</sup>, A. Krishna<sup>1</sup>, A. Trivedi<sup>1</sup>, R. Bhujel<sup>2</sup>, S. Rai<sup>2</sup>, I. Shivakoti<sup>1\*</sup> and K. Kalita<sup>3</sup>

\*ishwar.siwa@gmail.com

Received: May 2019

Revised: July 2020

Accepted: August 2020

<sup>1</sup> Department of Mechanical Engineering, Sikkim Manipal Institute of Technology, Sikkim Manipal University, Majitar, Rangpo-East Sikkim, India

<sup>2</sup> Center for Material Science and Nanotechnology, Sikkim Manipal Institute of Technology, Sikkim Manipal University, Majitar, Rangpo-East Sikkim, India

<sup>3</sup> Vel Tech Rangarajan Dr. Sagunthala R&D Institute of Science and Technology, Avadi, Chennai

DOI: 10.22068/ijmse.17.4.25

**Abstract:** Graphene oxide (GO) and reduced graphene oxide (rGO) is a semiconductor device which finds many applications in the various electronic devices. In the present study GO and rGO thin sheets have been grown over Si wafers using Hummer's and modified Hummer's methods and a comparison in the properties of the coatings have been carried out. The morphology of the sheets characterized by SEM revealed similar transparent sheet like structure for both methods of synthesis. The diffraction patterns of GO and rGO prepared with modified Hummer's method showed peak shift to lower diffraction angle from 9.96° to 9.63° and 26.4° to 26.3° respectively. The diffraction peaks were observed at diffraction phase of 001 and 002 crystal plane. FTIR spectra revealed presence of oxygen functional groups in GO thin sheets whereas peaks for oxygen functionalities were absent in rGO. The polarization curve indicated similar corrosion resistance of GO and rGO thin sheets grown under Hummer's and modified Hummer's. Capacitive property of rGO is better than GO as observed by the electrochemical analysis of GO and rGO.

**Keywords:** SEM, Hummer method, Graphene oxide.

## 1. INTRODUCTION

The application of graphene [1] in electronic devices with a single layer of graphite has received much attention among many research groups in the recent years. Graphene is a semiconductor device with 0 eV band gap where the already filled valence bands touches the unoccupied conduction band give rise to various electronic properties [2] having very wide applications in various electronic devices [3-6]. The fabrication of various devices on graphene sheets has become a straightforward process due to mechanical cleaving scotch tape method [1]. Various research groups have reported the growth of large area epitaxial graphene suitable for various industrial applications [7, 8]. In recent years, various research groups have reported many optimistic approaches such as transfer printing of exfoliated graphene onto electrodes and many more for different types of product basically for large scale integration [9-11]. Research groups, not only restricted themselves to individual sheet devices, but also various successful attempts have been reported regarding the development of graphene-

based composites by reducing graphene oxide (GO) using various solution and its successful incorporation into different hosts [12]. In recent studies it has been observed that large number of research groups have reported reduction of non-composite GO into graphene by employing various chemical routes and high-temperature annealing [13-17]. The various chemical approaches for the synthesis of graphene from different chemical solutions has made its fabrication way too easy on virtually any surface. rGO is synthesised either using chemical reduction or reduction through thermal process. But in most of the cases chemical reduction is preferred over thermal reduction as thermal reduction requires higher temperatures [18]. rGO is formed by successful reduction of GO. When reduced, rGO has structure similar to GO but the oxygen groups are removed. According to C. Gomez et al, the occurrence of hexagonal pattern in rGO indicates that there is a long range of hexagonal orientation in the sheets [19]. The applications of reduced graphene oxide are widely spread in many areas like chemical sensors and biosensors in Field Effect Transistor (FET) as a semiconductor which

is use for detection of hormonal catecholamine molecules. The transparent electrodes rGO's are being used as whole transparent layer for polymer cells and light emitting diodes (LED's) [20]. rGO has extremely high surface area which can be considered for electrodes, double-layered capacitors, fuel cells for solar cells [20]. Nano composites of rGO are being adsorbed by electrically insulating metal oxide nanoparticles for enhancing the efficiency of lithium ion batteries [21]. In this work, reduced GO layers over Si (100) substrate have been prepared using two different chemical routes namely Hummer's and modified Hummer's methods. The morphological, microstructural, tribological properties of the samples were further characterized through SEM, AFM, XRD, FTIR and by conducting corrosion test.

## 2. EXPERIMENTAL PROCEDURES

### 2.1. GO and rGO Synthesis Using Hummer's Method

2grams of graphite powder were mixed with 1 gram sodium nitrate ( $\text{NaNO}_3$ ) and 46ml of sulfuric acid (concentrated  $\text{H}_2\text{SO}_4$ ). The mixture was kept in ice-bath for an hour as the mixture was exothermic. After an hour 6 grams of potassium permanganate ( $\text{KMnO}_4$ ) was mixed in a gradual manner in the prepared solution. Further, the solution was taken out from the ice bath and the temperature was raised to 35 °C and was kept constant at that temperature. The solution was further stirred for 24 hours by using magnetic stirrer. After 24 hours 500ml of Deionized water was added and left for stirring for 1hr. Then at the end of the process 3ml of 30% hydrogen peroxide ( $\text{H}_2\text{O}_2$ ) was added. Then the solution was kept for filtration and drying. The rGO was synthesized using 0.2 gm of GO and sirriied with 50ml of deionized water for 90 minutes. The solution was heated at 90°C for 1 hour after addition of 2 ml of Hydrazine. Then the solution was kept for filtration and drying.

### 2.2. Synthesis of GO and rGO Using Modified Hummer's Method

Graphene Oxide was synthesized by mixing sulfuric acid ( $\text{H}_2\text{SO}_4$ -27ml of) and phosphoric acid ( $\text{H}_3\text{PO}_4$ -3ml). The acid mixture was stirred for one hour. After successful stirring graphite powder up to 0.225 grams was incorporated in the solution. Further, potassium permanganate

( $\text{KMnO}_4$ ) in 1.32 grams was added in a very slow manner in the solution. The mixture was stirred for 6 hours until the dark green colour solution was obtained. Further the elimination process of potassium permanganate was carried out by the gradual incorporation of hydrogen peroxide ( $\text{H}_2\text{O}_2$  -0.675 ml) for 10 minutes. An exothermic reaction had occurred and was left for cooling down. Once the cooling process is over, 10ml of hydrochloric acid (HCl) and 30ml of de-ionized water was added. Then the solution was left for filtration and drying. The synthesis of rGO using modified hummer method has been carried out using same procedure as in case of synthesis through hummers method. However, the chemicals and reagent used for synthesis of GO using Modified Hummer's Method are sulfuric acid ( $\text{H}_2\text{SO}_4$ ), potassium permanganate ( $\text{KMnO}_4$ ), hydrogen peroxide ( $\text{H}_2\text{O}_2$ ), phosphoric acid ( $\text{H}_3\text{PO}_4$ ), graphite powder, hydrochloric acid (HCl), and deionized water.

### 2.3. Characterization of GO and rGO Samples Prepared from Hummer's and Modified Hummer's Method

The morphology of rGO samples was analysed using scanning electron microscope and atomic force microscopy with model JSM-7600F with a resolution of 1 nm and Innova SPM AFM instrument with a scanner of 100  $\mu\text{m}$ . The structural properties of the prepared samples have been studied using XRD with model Rigaku Miniflex 600 (5th gen.). The X-Ray generation was up to 40 kV with a current of 15 mA. All tests were carried out at room temperature with Ni filters. The 2 $\theta$  values were recorded from 0°-80° XRD is done when monochromatic X-Rays, which are generated by cathode ray tube, are directed to fall on the sample. The atomic weight percentage of carbon and oxygen were measured through EDS technique using EVO MA18 with Oxford EDS(X-act) instrument with a maximum magnification factor of 10000x. The electrochemical corrosion resistance of the deposited samples has been evaluated using CH instrument Inc. (Electrochemical Analyser CHI608E) in presence of Ag/AgCl as a reference electrode, platinum wire as counter electrode and GO, rGO samples as working electrode. The solution used for electro chemical analysis was composed of 0.5M  $\text{H}_2\text{SO}_4$  solution.

### 3. RESULTS AND DISCUSSIONS

Figs.1 and 2 shows the SEM and EDS results of deposited samples synthesized by Hummers and modified Hummers methods. The SEM images show the formation of transparent sheet like structure for both GO and rGO. The sheets of GO have wrinkled shape and are stacked one upon other as clearly shown from Fig. 1 [22]. While in case of rGO the sheets are highly smooth, transparent and wrinkle free. The stacking and curling of carbon sheet is caused due the presence of excessive number of functional groups containing oxygen in GO. These functional groups are capable of forming H-bonds with the other nearest functional groups present within the GO and rGO sheet. This interaction between the functional groups present in different sheets causes stacking and

interaction within the same sheet causes the twisting and curling of GO sheets [23]. Similar results were also obtained for the GO and RGO synthesized by modified Hummers method. The EDS results confirm the presences of different elements in both GO and rGO. In case of GO the presence of other elements shown in figs. 1a and 2 is due to use of various oxidizing agents like  $H_2SO_4$ ,  $KMnO_4$ ,  $NaNO_3$ ,  $H_3PO_4$  in order to oxidize the graphite powder. Therefore, even after following the proper cleaning procedure traces of these elements remains in GO. In the next step the same GO as prepared earlier was reduced to form reduced graphene oxide. The as synthesized RGO is cleaned again with hot water, dil.HCl and ethanol which further remove the impurities left in RGO. The percentage of different atoms in the GO and RGO samples are given in table 1.

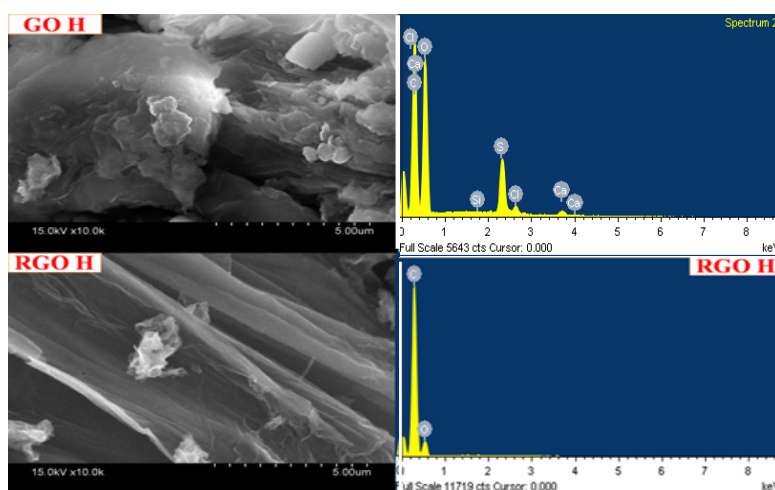


Fig. 1. SEM and EDS analysis of GO and rGO synthesized using Hummer's Method.

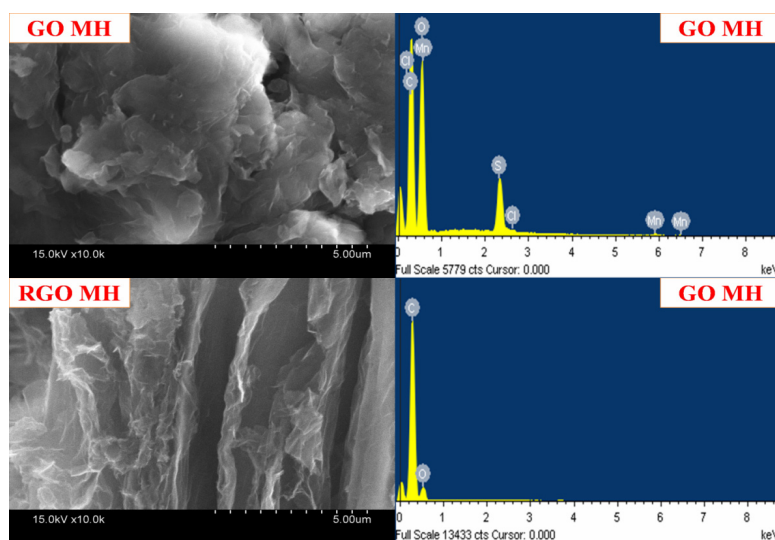


Fig. 2. SEM and EDS analysis of GO and rGO synthesized using Modified Hummer's Method.

**Table 1.** EDX Results for Graphene Oxide and Reduced Graphene Oxide

Element	C %	O %	S %	Cl %	Mn %	Si %
GO (Hummer's)	52.89	43.99	2.44	0.36	0	0.05
RGO (Hummer's)	81.4	18.6	0	0	0	0
GO (Modified Hummer's)	51.49	45.94	2.27	0.12	0.18	0
RGO (Modified Hummer's)	83.47	16.53	0	0	0	0

### 3.1. Structural Analysis by XRD

The Fig. 3 represents the XRD patterns of GO and rGO synthesized using Hummer's Method and Modified Hummer's Method. The  $2\theta$  diffraction pattern of rGO was observed at  $26.3^\circ$  and  $24.64^\circ$  with the phase of (002), while for GO it was found that  $2\theta$  values were  $9.96^\circ$  and  $9.63^\circ$  with a phase of (001) and (002) respectively. The presence of XRD pattern at  $9.96^\circ$  confirms the successful formation of GO, while in case of RGO a single band at  $\sim 24.6^\circ$  is observed confirming the reduction of GO to RGO.

The interlayer spacing between the GO and RGO sheets were calculated using the formula

$$d = \frac{n\lambda}{2\sin\theta} \quad (1)$$

Where,  $d$  is interlayer spacing in nm,  $\lambda$  is the wavelength of X-ray and  $\theta$  refers to the diffractin

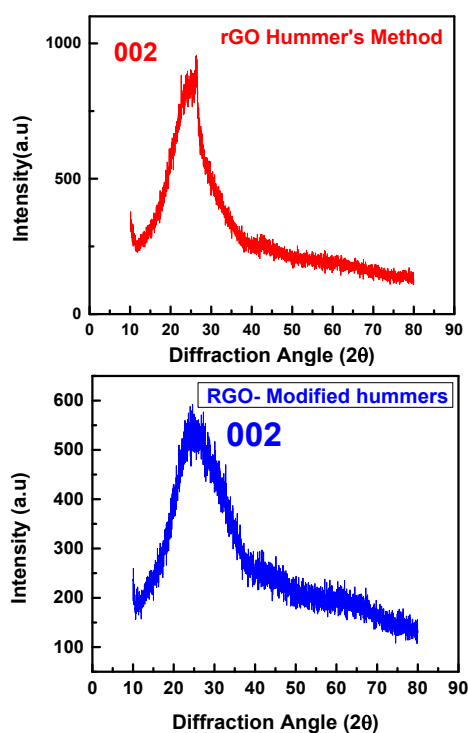


**Fig. 3.** XRD analysis of GO and rGO synthesized by Hummer's and Modified Hummer's method.

angle. It was found that the interlayer spacing for GO synthesized using Hummer's and Modified Hummer's method are 0.89 nm and 0.918 nm respectively, while for rGO synthesized using Hummer's and Modified Hummer's method are 0.34 nm and 0.36 nm respectively. The interlayer spacing in GO is high due to the presence of oxygen molecules between the graphene sheets, while in case of rGO the interlayer spacing is less because the number of oxygen atoms are reduced and at the same time the  $\pi$ - $\pi$  interaction between the two graphene sheet increases [24], which is responsible for the reduction in interlayer spacing between the RGO sheets. The difference in interlayer spacing is also due to weaker van der Waals bonding formed due to epoxy, hydroxyl, carbonyl and carboxyl group [24]. In earlier research report the interlayer spacing of GO is reported in the range of 0.6-1nm [25].

### 3.2. FTIR Analysis of GO and rGO

Fig. 4 shows the FTIR spectra for GO and rGO. The FTIR signatures for GO are obtained at 3312.2, 1722.2 and 1175.5  $\text{cm}^{-1}$  corresponds to the presence of -O-H, -C=O and C-O stretching vibrations in GO. The presence of a FTIR signal at 1617.3  $\text{cm}^{-1}$  is due to the C=C stretching of the  $\text{sp}^2$  hybridized ring carbon atoms. Moreover the peaks obtained at 1414 and 874.69  $\text{cm}^{-1}$  confirms the presence of C-H bonds in GO. The FTIR spectrum of rGO shows the absence of intense peaks for the oxygen functional groups, only a small peak at around 1722.2  $\text{cm}^{-1}$  is present for the C=O groups. Hence, from the FTIR analysis it is clear that GO is reduced to rGO.

### 3.3. Corrosion Behaviour of GO and rGO Grown by Hummer's and Modified Hummer's Method

Fig. 5 shows the polarization curve of GO and rGO through Tafel Plot by using GO - coated glassy carbon electrode and rGO- coated glassy carbon electrode. The polarization curve tells about the corrosion potential ( $E_{\text{corr}}$ ) and corrosion

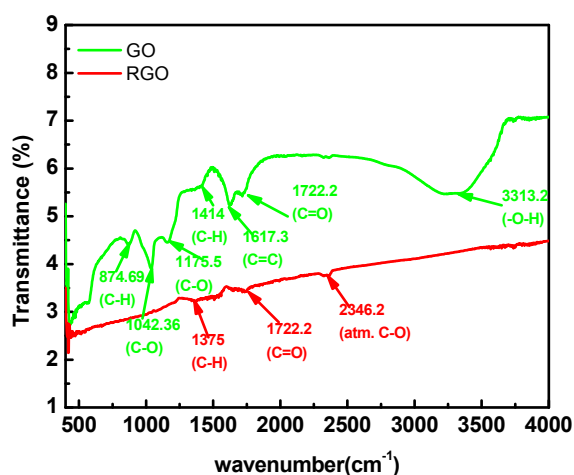


Fig. 4. FTIR spectra for GO and rGO.

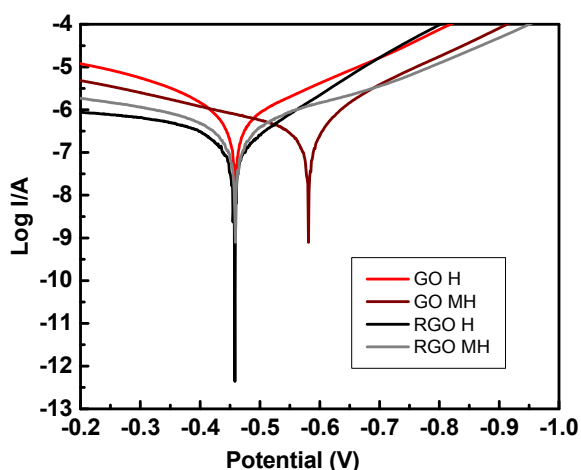


Fig. 5. Tafel Plot of rGO synthesized via Hummer's and Modified Hummer's Method.

current density ( $I_{corr}$ ) for various electrodes.  $E_{corr}$  and  $I_{corr}$  for GO synthesized using hummers method were found to be  $-0.459V$  and  $-9.11 A/cm^2$ . Similarly, for GO synthesized using Modified Hummer's  $E_{corr}$  was  $-0.58V$  and  $I_{corr}$  was  $-9.06VA/cm^2$ , for rGO Hummer's  $E_{corr}$  was  $-0.459 V$  and  $I_{corr}$  was  $-12.39 A/cm^2$  and for rGO synthesized using Modified Hummer's  $E_{corr}$  was  $-0.458V$  and  $I_{corr}$  was  $-9.135 A/cm^2$ . The corrosion resistivity of all sample are almost same i.e.  $-0.459 V$  except for GO synthesized from modified Hemmers method, which is  $-0.58 V$ . This is caused due to the presence of more number of impurity atoms like Na, S, Cl, Mn which are highly reactive with the acidic solution, therefore they tend to corrode at a faster rate. From the above corrosion test analysis we can conclude that GO and RGO samples shows similar corrosion resistivity against the acidic solutions Fig. 6 Shows cyclic

voltammetry curves of GO and RGO samples taken in  $1M H_2SO_4$  solution. The CV curves are almost rectangular shaped for both the GO and RGO samples with a very small oxidation peak at  $\sim 0.9 V$  in case of GO. The shape of the CV curve suggests that the capacitive behaviour of GO and RGO is due to the double layer capacitance. The presence of a oxidation peak in case of GO is due to the hydroquinone to quinone transformation in GO. NO such peaks for the CV curve of rGO is obtained, which implies a very good reduction of oxygen functional groups of GO. The specific capacitance of GO and rGO was further calculated by applying the formula

$$C_m = \frac{1}{mv(V_b - V_a)} \int_{V_a}^{V_b} IdV \quad (2)$$

Where  $C_m$  the specific capacitance in  $Fg^{-1}$  is,  $m$  is the mass of electroactive surface,  $v$  is the scan rate in  $Vs^{-1}$ ,  $(V_b-V_a)$  denotes potential window and  $I$  is the integrated area under the CV curve. The maximum value of specific capacitance was  $116.67 Fg^{-1}$  achieved by RGO (MH) which is due to the quality improvement of rGO sheet. The specific capacitance of RGO (H) is  $\sim 23.25 Fg^{-1}$  which shows similarity with the previously reported work by [22]. For GO (H) and GO (MH) the  $C_m$  values were very poor as given in table 2. The improvement in capacitance for RGO is due to the reduction of oxygen containing functional groups of GO sheet and also due to the improvement of the C=C bond in ring carbon atoms. On comparing the values of specific capacitance, RGO(H) showed higher capacitance value of  $116.67 F/g$  while the capacitance obtained from RGO (MH) i.e.  $23.25 F/g$  at a scan rate of  $0.01 V/s$ .

### 3.4. Electrochemical Impedance Spectroscopy Study of GO and RGO

Fig. 7 shows the Nyquist plot of GO and RGO samples. The schematic of circuit diagram shown in Fig.8 represents  $R_e$  as the electrolytic resistance,  $R_{CT}$  as charge transfer resistance,  $W$  represents Warburg impedance and  $Cdl$  corresponds to the double layer capacitance. The Nyquist plot of GO and rGO shows a semicircle which corresponds to the charge transfer resistance. The value of charge transfer resistance for GO  $345\Omega$  for modified Hummer's and  $223.8\Omega$  for Hummer's. The value of charge

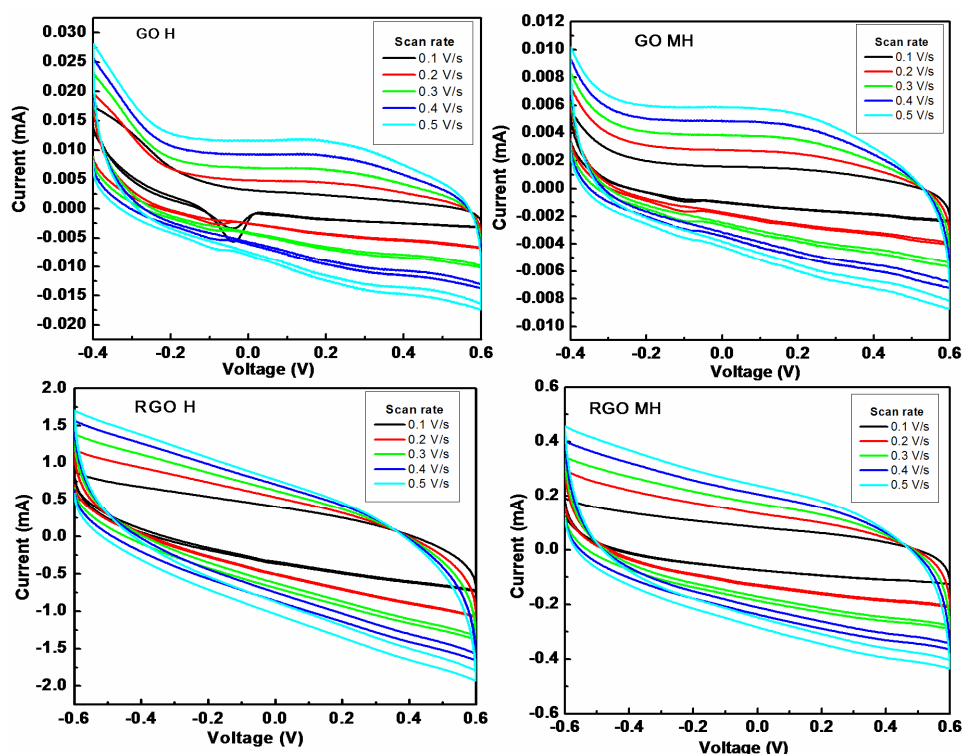


Fig. 6. Supercapacitive properties of GO and RGO synthesized by Hummer's and Modified Hummer's method.

Table 2. Specific Capacitance of GO and rGO synthesized by Hummer's and Modified Hummer's method at different scan rates.

Sample	Capacitance in F/g				
	0.1V/s	0.2V/s	0.3V/s	0.4V/s	0.5V/s
GO (H)	1.01	0.67	0.62	0.48	0.60
GO (MH)	0.43	0.35	0.32	0.30	0.28
RGO (H)	116.67	79.16	66.67	58.33	55.00
RGO (MH)	23.25	19.33	17.08	15.83	14.91

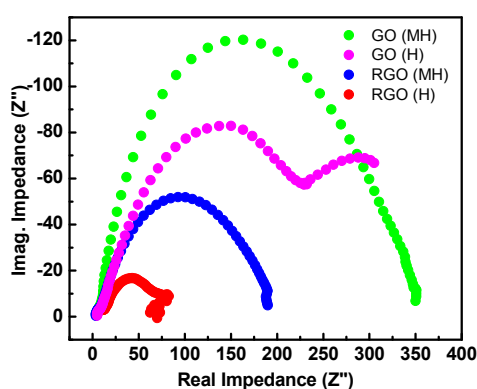


Fig. 7. Nyquist plot of GO and RGO samples.

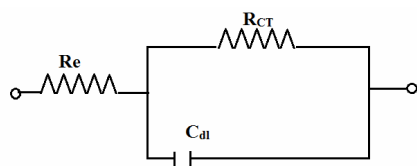


Fig. 8. Circuit Diagram.

transfer of rGO synthesized by reducing GO MH is  $185\Omega$  and  $64.7\Omega$  respectively. The small  $R_{CT}$  of rGO corresponds to the decrease in charge transfer resistance and hence increase in conductivity. These values are in favour of the CV results shown above in Figs. 5. Fig 8 shows the circuit diagram. The value of charge transfer resistance RGO (MH) is  $185\Omega$  and for RGO(H) it is  $64.7\Omega$  respectively. Because of the greater charge transfer resistance of RGO (MH), it has lesser value of capacitance.

#### 4. CONCLUSION

In the present work, structural and electrochemical properties of GO and rGO synthesized by Hummer's and Modified Hummer's methods have been compared. SEM results revealed transparent sheet like structure for

both GO and rGO synthesized by both methods. The EDS result showed successful reduction of oxygen atoms for rGO sheets. Results also revealed higher amount of oxygen reduction of rGO (MH) than rGO (H). The GO and rGO diffraction pattern were observed within  $9.63^\circ$  to  $9.96^\circ$  and  $26.3^\circ$  to  $24.64^\circ$  respectively. The single band of rGO observed  $24.64^\circ$  confirmed successful reduction of GO to rGO. The interlayer spacing of GO (MH) and rGO (MH) found to be increased in comparison to GO (H) and rGO (H). FTIR spectra revealed  $\text{-O-H}$ ,  $\text{-C=O}$  and  $\text{C-O}$  stretching vibrations in GO at  $3312.2\text{ cm}^{-1}$ ,  $1722.2\text{ cm}^{-1}$  and  $1175.5\text{ cm}^{-1}$ , whereas no peaks of oxygen functional group was observed in the FTIR spectra of rGO. The corrosion resistance of GO(H), rGO (H) and rGO (MH) found to be similar whereas GO (MH) showed reduced corrosion resistance. The specific capacitance of rGO (MH) showed better results than GO (MH) due to improvement in rGO sheet. Electrochemical impedance spectroscopy results revealed higher conductivity of rGO samples compared to GO samples.

## REFERENCES

1. Novoselov, Kostya S., Andre K. Geim, Sergei V. Morozov, D. Jiang, Y. Zhang, Sergey V. Dubonos, Irina V. Grigorieva, and Alexandr A. Firsov. "Electric field effect in atomically thin carbon films." *Science*, 2004, 306, 666-669.
2. Geim, A. K. and Novoselov, K. S., "The rise of graphene". *Nature Mater.*, 2007, 6, 183 – 19. Doi:10.1142/9789814287005\_0002
3. Schedin, F., Geim, A.K., Morozov, S.V., Hill, E.W., Blake, P., Katsnelson, M.I. and Novoselov, K.S., "Detection of individual gas molecules adsorbed on graphene". *Nature Mater.*, 2007, 6, 652–655. Doi: 10.1038/nmat1967
4. Han, M. Y., Ozyilmaz, B., Zhang, Y. B., and Kim, P., "Energy band-gap engineering of graphene nanoribbons", *Phys. Rev. Lett.*, 2007, 98, 20680. Doi: 10.1103/PhysRevLett.98.206805
5. Barbolina, I.I., Novoselov, K.S., Morozov, S.V., Dubonos, S.V., Missous, M., Volkov, A.O., Christian, D.A., Grigorieva, I.V. and Geim, A.K., "Submicron sensors of local electric field with single-electron resolution at room temperature". *Appl. Phys. Lett.*, 2006, 88, 01390. Doi:10.1063/1.2159564
6. Tombros, N., Jozsa, C., Popinciuc, M., Jonkman, H. T. and van Wees, B. J., "Electronic spin transport and spin precession in single graphene layers at room temperature". *Nature*, 2007, 448, 571 –574. Doi:10.1038/nature06037
7. Berger, C., Song, Z., Li, T., Li, X., Ogbazghi, A.Y., Feng, R., Dai, Z., Marchenkov, A.N., Conrad, E.H., First, P.N. and De Heer, W.A., "Ultrathin epitaxial graphite: 2D electron gas properties and a route toward graphene based nanoelectronics", *J. Phys. Chem. B*, 2004, 108, 19912–19916. Doi:10.1021/jp040650f
8. Coraux, J., N'Diaye, A. T., Busse, C. and Michely, T., "Structural coherency of graphene on Ir(111)", *Nano Lett.*, 2008, 8, 565 –570. Doi:10.1021/nl0728874
9. Liang, X., Fu, Z. and Chou, S. Y., "Graphene transistors fabricated via transfer-printing in device-active areas on large wafer", *Nano Lett.*, 2007, 7, 3840–3844. Doi: 10.1021/nl072566s
10. Chen, J - H., Masa Ishigami, Chaun Jang, Daniel R. Hines, Michael S. Fuhrer, and Ellen D. Williams, "Printed graphene circuits", *Adv. Mater.*, 2007, 19, 3623–3627. Doi: 10.1002/adma.200701059
11. Meitl, M.A., Zhu, Z.T., Kumar, V., Lee, K.J., Feng, X., Huang, Y.Y., Adesida, I., Nuzzo, R.G. and Rogers, J.A., "Transfer printing by kinetic control of adhesion to an elastomeric stamp" .*Nature Mater.*, 2006, 5, 33 –38. Doi: 10.1038/nmat1532
12. Stankovich, S., Dikin, D.A., Dommett, G.H., Kohlhaas, K.M., Zimney, E.J., Stach, E.A., Piner, R.D., Nguyen, S.T. and Ruoff, R.S., "Graphene-based composite materials", *Nature*, 2006, 442, 282–286. Doi: 10.1038/nature04969
13. Gómez-Navarro, C., Weitz, R.T., Bittner, A.M., Scolari, M., Mews, A., Burghard, M. and Kern, K., "Electronic transport properties of individual chemically reduced graphene oxide sheets", *Nano Lett.*, 2007, 7, 3499–3503. Doi:10.1021/nl072090c
14. Gijie, S., Han, S., Wang, M., Wang, K. L. and Kaner, R. B., "A chemical route to graphene for device applications", *Nano Lett.*, 2007, 7, 3394–3398. Doi: 10.1021/nl0717715

15. Wang, X., Zhi, L. and Mullen, K., "Transparent, conductive graphene electrodes for dye-sensitized solar cells", *Nano Lett.*, 2007, 8, 323–327. Doi: 10.1021/nl072838r
16. Schniepp, Hannes C., Je-Luen Li, Michael J. McAllister, Hiroaki Sai, Margarita Herrera-Alonso, Douglas H. Adamson, Robert K. Prud'homme, Roberto Car, Dudley A. Saville, and Ilhan A. Aksay., "Functionalized single graphene sheets derived from splitting graphite oxide", *J. Phys. Chem. B*, 2006, 110, 8535–8539. Doi:10.1021/jp060936f
17. McAllister, M.J., Li, J.L., Adamson, D.H., Schniepp, H.C., Abdala, A.A., Liu, J., Herrera-Alonso, M., Milius, D.L., Car, R., Prud'homme, R.K. and Aksay, I.A., "Single sheet functionalized graphene by oxidation and thermal expansion of graphite", *Chem. Mater.*, 2007, 19, 4396–4404. Doi: 10.1021/cm0630800
18. Du, J. and Cheng, H.M., "The fabrication, properties, and uses of graphene/polymer composites", *Macromolecular Chemistry and Physics*, 2012, 213(10 - 11), 1060-1077. Doi: 10.1002/macp.201200029
19. Gómez-Navarro, C., Meyer, J.C., Sundaram, R.S., Chuvilin, A., Kurasch, S., Burghard, M., Kern, K. and Kaiser, U., "Atomic structure of reduced graphene oxide", *Nano letters*, 2010, 10(4) 1144-1148. Doi: 10.1021/nl9031617
20. Lu, G., Park, S., Yu, K., Ruoff, R.S., Ocola, L.E., Rosenmann, D. and Chen, J., "Toward practical gas sensing with highly reduced graphene oxide: a new signal processing method to circumvent run-to-run and device-to-device variations", *ACS nano*, 2011, 5(2), 1154-1164. Doi: 10.1021/nn102803q
21. Wang, H., Cui, L.F., Yang, Y., Sanchez Casalongue, H., Robinson, J.T., Liang, Y., Cui, Y. and Dai, H., "Mn<sub>3</sub>O<sub>4</sub>- graphene hybrid as a high-capacity anode material for lithium ion batteries", *Journal of the American Chemical Society*, 2010, 132(40), 13978-13980. Doi: 10.1021/ja105296a
22. Bhujel, R., Rai, S. and Swain, B.P., "Investigation of cyclic voltammetry, impedance spectroscopy and electrical properties of thermally exfoliated biomass-synthesized graphene" *Appl Nanosci*, 2019, 9, 1319-1331. Doi: 10.1007/s13204-018-00944-9
23. Vijapur SH, Wang D, Ingram DC, Botte GG, "An investigation of growth mechanism of coal derived graphene films" *Mater Today Commun*, 2017, 11,147–155. Doi: 10.1016/j.mtcomm.2017.04.003
24. Rai, S., Bhujel, R. and Swain, B.P., 2018, "Electrochemical Analysis of Graphene Oxide and Reduced Graphene Oxide for Super Capacitor Applications", *IEEE Electron Devices Kolkata Conference (EDKCON)*, 2018, 489-492.
25. Sheng, Y., Tang, X., Peng, E. and Xue, J., "Graphene oxide based fluorescent nanocomposites for cellular imaging", *Journal of Materials Chemistry B*, 2013, 1(4) 512-521.